1985

Vision Res. Vol. 25, No. 12, pp. 1811–1827, 1985
Printed in Great Britain.

0042-6989/85 $3.00 + 0.00

COMPLEX VISUAL TEXTURES AS A TOOL FOR STUDYING THE VEP

JONATHAN D. VICTOR
Laboratory of Biophysics, The Rockefeller University, 1230 York Avenue, New York, NY 10021-6399 and Department of Neurology, New York Hospital-Cornell Medical Center, New York, N.Y., U.S.A.

(*Received* 31 *December* 1984; *in revised form* 7 *May* 1985)

Abstract—A method of separating components of the visual evoked potential by using complex visual textures is described. Interchange of visual textures with identical power specta and third-order autocorrelations elicits a response which may be analyzed into symmetric and asymmetric components. It is shown that the asymmetric component depends on complex attributes of form. Mechanisms that generate this component must possess nonlinear interactions among multiple areas of the visual pattern. These interactions are likely to be more complex than rectification following spatial summation. It is concluded that the asymmetric component reflects intracortical, rather than precortical, processsing.

Visual evoked potentials Systems analysis Parallel visual processing Feature analysis Human

INTRODUCTION

Visual processing requires many transformations, both sequential and parallel, distributed among many neuronal groups. Each step in this processing is a possible contributor to the visual evoked potential (VEP). The size and character of the contribution depends on several factors: the excitatory or inhibitory nature of the cellular processes (Creutzfeldt and Kuhnt, 1973; Creutzfeldt *et al.*, 1969; Zemon *et al.*, 1980; Nakayama, 1982) the geometry of the neurons involved (Jeffreys and Axford, 1972a, b; Lehmann *et al.*, 1982; Vaughan, 1982), and the passive electrical properties of the brain (Nunez, 1981).

A fuller understanding of the components of the VEP would further its utility as a research and clinical tool (Regan, 1972; Spekreijse *et al.*, 1977; Celesia, 1982; Chiappa and Ropper, 1982). One established physiological approach to this problem is to manipulate the stimulus pattern so that visual neurons with differing receptive-field properties will be selectively stimulated. For example, Tyler and coworkers used gratings with a range of spatiotemporal characteristics to demonstrate sharp spatiotemporal tuning of VEP components (Tyler *et al.*, 1978; Tyler and Apkarian, 1982). Spekreijse and coworkers (1973, 1977) manipulated spatial and temporal aspects of the standard checkerboard stimulus to determine that a local contrast signal, as well as a luminance signal, must participate in the generation of the VEP. Their data imply neural spatial summation prior to a rectifier-like stage. Zemon and Ratliff (1982, 1984) have used complex spatiotemporal patterns to dissect out a VEP component that reflects a kind of lateral interaction, whose characteristics strongly suggest a cortical origin.

This study is a further investigation of lateral interactions as manifest in the VEP. The visual stimuli consist of a class of complex textures, called isodipole textures, with several remarkable symmetry properties (Julesz *et al.*, 1978). With these textures, it is possible to manipulate independently local contrast, spatial frequency spectra, and more complex attributes of pattern (Victor and Zemon, 1984). This freedom allows a separation of lateral interactions into components that rely on local contrast and therefore may be generated by relatively simple mechanisms (e.g. retinal or early cortical processing) and components that are independent of local contrast and require quite complex spatial interactions. This refinement may lead to a fuller understanding of the processes that generate the VEP, analogous to the refinements in understanding provided by the use of simple patterns.

The theoretical basis of this approach to the dissection of components of the VEP rests on the statistical properties of the ensemble of isodipole visual textures. Reduction of this method to practice requires the demonstration that particular members of the ensemble of textures have statistics that typify those of the ensemble.

This sets forth the theoretical basis of this approach, and its reduction to practice. In man, this technique isolates a VEP component that reflects complex lateral interactions. The qualitative features of a minimal model of cortical processing that can produce such a response are discussed. These findings are compared with the results of other methods of analyzing the VEP. In another paper (Victor and Zemon, 1985), the dependence of the responses on the contrast, correlation structure, scale, and modulation frequency of the isodipole stimuli is explored. This allows further evaluation of models of cortical interactions and the genesis of the VEP.

STIMULUS DESCRIPTION

The visual stimuli used in these experiments are based on an "isodipole texture pair" introduced by Julesz *et al.* (1978) to study texture perception. In this section, the construction of these textures, their relevant properties, and their use in evoked potential experiments will be described. The reader interested in the mathematical details should consult Appendix A.

Definition of the textures

The basic textures consist of a pair of colorings of a black and white square lattice. Denote the cell in the ith row and jth column by $A_{i,j}$. Let its color be given by $a_{i,j}$, where $a_{i,j} = -1$ indicates that the cell is black and $a_{i,j} = +1$ indicates that the cell is white. The textures are defined recursively in the following way: color the cells $A_{0,j}$ and $A_{i,0}$ in the initial (zeroth) row and column black and white at random. That is, $a_{0,j}$ and $a_{i,0}$ each have a probability of 0.5 of being either -1 or $+1$, and are all uncorrelated.

For each of the two textures, a rule determines the intensity of the interior cells ($A_{i,j}$, $i > 0$ and $j > 0$) from those previously colored. This construction is illustrated in Fig. 1.

$$\text{Even texture:} \quad a_{i,j} = a_{i-1,j} \cdot a_{i,j-1} \cdot a_{i-1,j-1}$$

$$\text{Odd texture:} \quad a_{i,j} = a_{i-1,j} \cdot a_{i,j-1} \cdot a_{i-1,j-1}. \qquad (1)$$

Thus, every 2×2 block of cells of the even texture contains an even number (0, 2, or 4) of both black and white cells, and every 2×2 block of cells of the odd texture contains an odd number (1 or 3) of both black and white cells.

It remains to specify the initial row and column. For most of the experiments described here, shift register sequences of order k (Golomb, 1968) were used to dictate the "random" choice of the colors of the cells $A_{0,j}$ and $A_{i,0}$ in the initial row and column (Table 1). This procedure approximately balances the texture for occurrences of all of the possible $k \times k$ blocks. Further details are discussed in Appendix B.

Properties of the textures

It may be shown that the recursive rules [equation (1)] are equivalent to the following rules, which determine the intensity of an interior cell from the intensities of three cells on the texture's boundary (Julesz *et al.*, 1978; Appendix A)

$$\text{Even texture:} \quad a_{i,j} = a_{i,0} \cdot a_{0,j} \cdot a_{0,0}$$

$$\text{Odd texture:} \quad a_{i,j} = a_{i,0} \cdot a_{0,j} \cdot a_{0,0} \cdot (-1)^{ij}. \qquad (2)$$

This key relation has several important consequences:

(I) In both textures, the intensities of two cells a fixed distance apart are uncorrelated. Thus, (IA) the autocorrelation of the two textures is identical, and equal to the autocorrelation of a randomly-colored checkerboard; (IB) the (spatial) power spectra of the textures, which are equal to the spatial Fourier transforms of their autocorrelations, are identical; and (IC) the average contour length per unit area of both textures are identical, since in each texture, any two neighboring cells have a probability of 0.5 of differing in intensity.

(II) In both textures, there are no third-order correlations between cells, and therefore any feature which distinguishes the textures must rely on nonlinear interactions involving at least four cells.

(III) In a statistical sense, both textures are homogeneous in the plane. Choosing different examples of each texture (different values for the starting row and column $a_{0,j}$ and $a_{i,0}$) is equivalent to translation of the origin.

(IV) For a given selection of intensities $a_{0,j}$ and $a_{i,0}$, the textures coincide at three-quarters of the cells

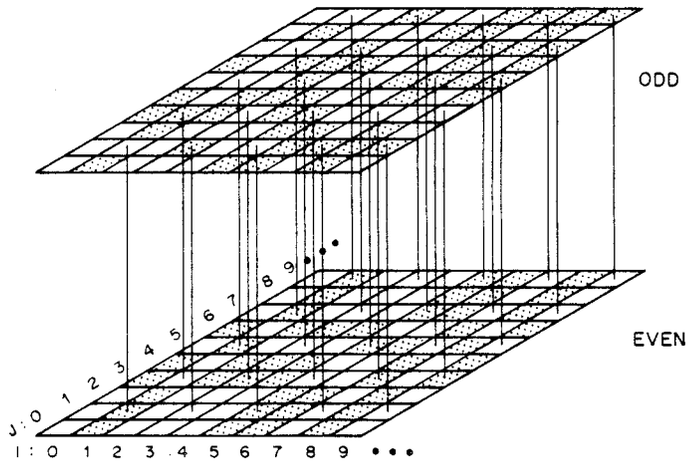

Fig. 1. A diagram of the construction of the "even" and "odd" textures. Each plane illustrates one of the two textures. Unfilled cells have a luminance above the mean; stippled cells have a luminance the same distance below the mean. Three-quarters of the cells are at the same luminance in both textures. The remaining quarter of the cells, at the intersection of an odd-numbered row and an odd-numbered column, are in opposite states. These cells are connected by the solid vertical ines.

Table 1. Initial row and column of stimuli derived from shift registers

Number of cells in map	Defining shift register	Initial row and column			
256 × 256	Initial row: $x^7 = x^3 + x^0$	+ + − + + − + +	+ + + + − + + +	− + + − − + + +	− + − − − + − +
		− − + − − + + +	+ + − − + + − −	+ − + − + + − −	− + + − − − − +
		− − + − + + + +	− + − + − + − −	− − − + − + + −	+ − + + + − − +
		− − − + + + − −	− − − − − + + +	+ − − − + − − −	− + + − + − − +
		+ − + + − + + +	+ + + − + + + −	+ + − − + + + −	+ − − − + − + −
		− + − − + + + +	+ − − + + − − +	− + − + + − − −	+ + − − − − + −
		− + − + + + + −	+ − + − + − − −	− − + − + + − +	− + + + − − + −
		− − + + + − − −	− − − − + + + +	− − − + − − − −	+ + − + − − + +
	column: $x^7 = x^1 + x^0$	+ − + − + + + −	− − − + + − + +	+ − + − − + + −	− − + − + − + +
		− − − − − + − +	+ + + − − − + +	+ − + + − + + −	− + − − + − + −
		− + − − − − + −	− + + + − − + −	+ + − + − − − +	− − − + + − − +
		+ − + − + − + −	− − − − − − + +	+ + + + − + + +	+ + − − + + + +
		− + − + + + − −	− − + + − + + +	− + − − + + − −	− + − + − + + −
		− − − − + − + +	+ + − − − + + +	− + + − + + − −	+ − − + − + − −
		+ − − − − + − −	+ + + − − + − +	+ − + − − − + −	− − + + − − + +
		− + − + − + − −	− − − − − + + +	+ + + − + + + +	+ − − + + + + −
128 × 128	Initial row: $x^6 = x^4 + x^3 + x^1 + x^0$	+ + − + + − − −	− + + + + + − −	+ − − − + + − −	+ + + − − − + −
		+ − − − − − − +	− − + − + + + −	+ + + + − + − −	+ + − + − + − +
		+ − + + − − − −	+ + + + + − − +	− − − + + − − +	+ + − − − + − +
		− − − − − − + −	− + − + + + − +	+ + + − + − − +	+ − + − + − + +
	column: $x^6 = x^1 + x^0$	+ − + − + + − −	− − + − + + + −	− − + + − + + −	+ − − + − − − +
		− − + + − − + −	+ − + − − − − −	− + + + + + − +	+ + + − − + + +
		− + − + + − − −	− + − + + + − −	− + + − + + − +	− − + − − − + −
		− + + − − + − +	− + − − − − − −	+ + + + + − + +	+ + − − + + + −
86 × 86	Initial row: $x^6 = x^4 + x^3 + x^1 + x^0$	− + + + + + − −	+ − − − + + − −	+ + + − − − + −	+ − − − − − − +
		− − + − + + + −	+ + + + − + − −	+ + − + − + − +	+ − + + − − − −
		+ + + + + − − +	− − − + + − − +	+ + − − − +	
	column: $x^6 = x^1 + x^0$	− + + + + + − +	+ + + − − + + +	− + − + + − − −	− + − + + + − −
		− + + − + + − +	− − + − − − + −	− + + − − + − +	− + − − − − − −
		+ + + + + − + +	+ + − − + + + −	+ − + + − −	
64 × 64 (EOSR4A)	Initial row: $x^5 = x^3 + x^2 + x^1 + x^0$	+ + − − + + + +	− + − − + − + −	+ + + − − − + −	− − − − + + − +
		+ − − + + + + −	+ − − + − + − +	+ + − − − + − −	− − − + + − + +
	column: $x^5 = x^2 + x^0$	+ − + − + + + +	− + + − + − − +	+ − − − − − + +	+ − − + − − − +
		− + − + + + + −	+ + − + − − + +	− − − − − + + +	− − + − − − + −
64 × 64 (EOSR4B)	Initial row: $x^5 = x^4 + x^2 + x^1 + x^0$	− + + − + − + −	− + + + + − − −	+ + − − + − − −	− − + − + + + −
		+ + − + − + − −	+ + + + − − − +	+ − − + − − − −	− + − + + + − +
	column: $x^5 = x^3 + x^2 + x^1 + x^0$	− − + + − − − −	+ − + + − + − +	− − − + + + − +	+ + + + − − + −
		− + + − − − − +	− + + − + − + −	− − + + + − + +	+ + + − − + − −
64 × 64 (EOSR4C)	Initial row: $x^5 = x^2 + x^0$	+ − + − + + + +	− + + − + − − +	+ − − − − − + +	+ − − + − − − +
		− + − + + + + −	+ + − + − − + +	− − − − − + + +	− − + − − − + −
	column: $x^5 = x^4 + x^2 + x^1 + x^0$	+ − − + − + − +	+ − − − − + + +	− − + + − + + +	+ + − + − − − +
		− − + − + − + +	− − − − + + + −	− + + − + + + +	+ − + − − − + −
43 × 43	Initial row: $x^5 = x^3 + x^2 + x^1 + x^0$	− + − + − + + +	− − − + − − − −	− + + − + + − −	+ + + + − + − −
		+ − + − + + + −	− − +		
	column: $x^5 = x^2 + x^0$	− + + − + − + −	− − − − + + + +	− + + + − − + +	− + − + − − − −
		− + + + + − + +	+ − −		
32 × 32	Initial row: $x^5 = x^3 + x^2 + x^1 + x^0$	− + + − + + − −	+ + + + − + − −	+ − + − + + + −	− − + − − − − −
	column: $x^5 = x^2 + x^0$	− + + + − + − +	− − − − + − − +	− + + − − + + +	+ + − − − + + −

These initial rows and columns define (through equation 2) the stimuli used in most of the experiments presented here. The three varieties of the 64 × 64 stimulus are used in Figure 4. A "+" indicates a cell above the mean luminance; a "−" indicates a cell below the mean luminance. For details, see Appendix B.

(those in an even-numbered row and an even-numbered column) and are of opposite intensity in the remaining one-quarter of the cells (at the intersection of an odd-numbered row and an odd-numbered column).

Use of the textures as visual stimuli

Property (IV) above is crucial for the present method of adapting the textures to VEP experiments. Even and odd textures may be interconverted by reversing the contrast (exchanging black for white and vice-versa) of the one-quarter of the squares at the intersection of an odd-numbered row and odd-numbered column, as illustrated in Fig. 1. In these experiments, this luminance modulation is sinusoidal. The remaining three-quarters of the stimulus are not modulated in time. Photographs of this stimulus in the even and odd configurations are shown in Fig. 2(A).

A simple but useful variation of the stimuli is obtained by replacement of the unmodulated (but patterned) portion of the stimulus by uniform light at

mean illumination. The resulting stimulus consists of a uniform gray background interrupted at regular intervals by square cells of light and dark [Fig. 2(B)]. These cells are modulated in counterphase, as in the original stimulus.

Although the two states of this modified stimulus are clearly different upon close inspection, the difference is far less striking than the difference between the two phases of the original stimulus [Fig. 2(A)]. This is because the modified stimuli share the same local features, although the exact spatial positions of these features have been scrambled. In other words, the two phases of the modified stimuli are drawn from the same ensemble. The original stimuli [Fig. 2(A)] are drawn from statistically different ensembles; but the distinguishing features depend on high-order correlations between the modulated and unmodulated portions of the texture.

METHODS

The stimuli described above were realized on a Tektronix 608 display oscilloscope with a fast (P31) phosphor. The X, Y, and Z voltages were generated by specialized electronics interfaced to a PDP 11/23 computer (Milkman *et al.*, 1980). This apparatus provided for control of a 256 × 256-pixel raster display at a frame rate of 270.3 Hz. The raster has a mean luminance of 154 cd/m^2, with the Z input of the oscilloscope modified so that luminance is linear as a function of voltage up to a contrast of at least 0.5. The display subtended an 8.8 × 8.8 deg region at the viewing distance of 57 cm. In all studies reported here, certain stimulus parameters were used: the cell size was 8.25 min (4 × 4 pixels), the contrast of unmodulated region and peak contrast of modulated region was 0.3, the modulation frequency was 4.19 Hz, and viewing was binocular.

Recordings were made in a darkened room, with the subject's head stabilized on a chinrest. Subjects were requested to fixate on a blackened point in the center of the display. All subjects were healthy adult volunteers (ages 29–60; five males and two females) with normal (with correction, if necessary) visual acuity and no neuro-ophthalmologic disease. The EEG was recorded using bipolar cup electrodes at C_z and O_z, using P_z as ground. After amplification and bandpass filtering (0.03–100 Hz), the computer averated the scalp signal over each stimulus cycle for 1-min episodes. In the averaged tracings reproduced here, upward deflection indicates negativity at O_z.

Fourier components of the responses were obtained at the input frequency and its first six harmonics. For the fundamental, a phase of zero means no lead or lag relative to the input signal. For the second harmonic, a phase of zero indicates no phase shift relative to the second harmonic component that would be contained in the square of the input. For both fundamental and second harmonics, negative phases denote a phase lag of the output relative to the above-defined reference phases.

RESULTS

In this section, the basic qualitative features of the VEP elicited by sinusoidal interchange of the isodipole stimuli will be presented. Then, experiments to explore the possible effects of inhomogeneities and restricted sampling of the stimulus ensemble will be described. These later experiments are important controls, allowing strong qualitative inferences regarding the nature of the neural mechanisms responsible for the VEP.

Responses to interchange of even and odd textures

The basic method underlying this approach to isolate VEP components is the use of a visual stimulus whose two configurations are designed to produce identical population activity among neurons with qualitatively linear receptive fields, and differing activity among a population of select neurons with more complex receptive field properties. Thus, the main feature of interest in the VEP elicited by interchange of the two stimulus configurations is whether the responses are symmetrical or not. A symmetrical response may be due to either linear or nonlinear receptive field mechanisms followed by simple rectification; an asymmetrical response must be due to complex nonlinear mechanisms (see Discussion).

Fourier analysis provides a convenient way to quantify the symmetric and asymmetric components of the response to texture interchange: second and higher even-order harmonics reflect components common to both textures, whereas fundamental and higher odd-order harmonics reflect response components that depend on differences between the textures.

Figure 3(A) shows a typical VEP elicited by sinusoidal modulation at 4.19 Hz of the standard stimulus [Fig. 2(A)]. The VEP is distinctly different in the two halves of the stimulus cycle. Fourier analysis quantifies these features: there is a large fundamental component (1.96 μV) and a smaller, but reliable, second-harmonic component (1.75 μV).

In Fig. 3(B), the contrast of the unmodulated portion of the stimulus is reduced to zero, so that the stimulus consists of transitions between the two configurations illustrated in Fig. 2(B). The resulting VEP is nearly identical in the two phases of the stimulus cycle. Accordingly, Fourier analysis no longer reveals a significant fundamental component, and the second-harmonic component is large (2.74 μV). Significantly, the phase of the second harmonic differs in the two conditions (−9 deg when the unmodulated region is at zero contrast, as compared with 164 deg for the full stimulus). For comparison with standard VEP studies, Fig. 3(C) shows the response to a sinusoidally-reversed checkerboard of identical check size. Again, only symmetric responses to the two configurations occur. For these conditions, the second-harmonic component

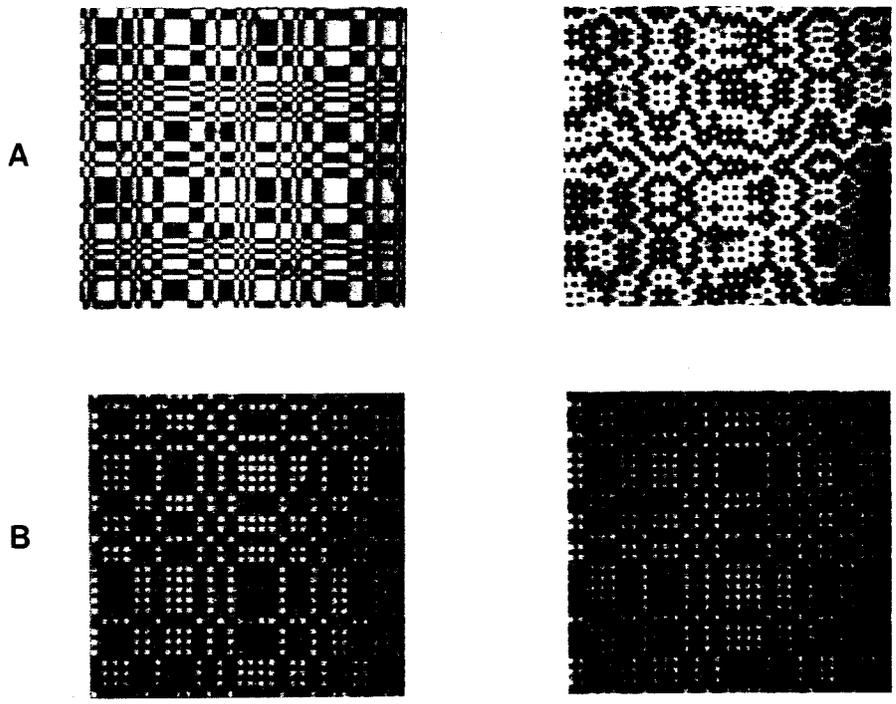

Fig. 2. Photographs of the "even" and "odd" configurations of some of the stimuli used. (A) The standard stimulus, with modulated and unmodulated portions at equal contrast. The even texture is on the left; the odd texture is on the right. (B) Unmodulated portion at zero contrast, and intensity equal to the mean intensity of the bright and dark squares. In (B) the two configurations are statistically indistinguishable.

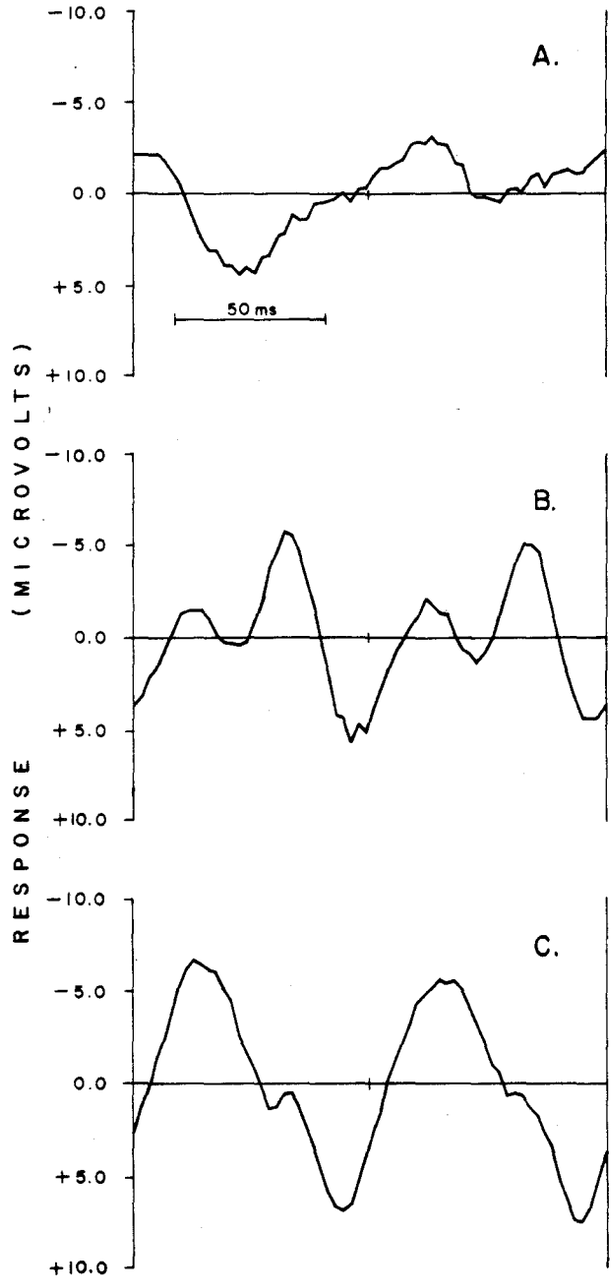

Fig. 3. (A) Steady-steate responses to sinusoidal interchange of even and odd textures at 4.19 Hz In (B), the contrast of the unmodulated region is reduced to zero. In (C), the stimulus is a contrast-reversing checkerboard. Subject: M.C.

(5.56 μV) is larger than the second-harmonic responses to the more complex stimuli, but this relationship varies from subject to subject.

Role of inhomogeneities

The previous experiments demonstrated an asymmetric response to the transitions between even and odd textures. This asymmetry required the presence of the unmodulated component of the pattern, which supports the notion that the asymmetric response reflects complex spatial interactions. Alternatively, one might suppose that nonuniformities of the stimulus, perhaps coupled with retinal inhomogeneities, generate the asymmetric component. That is, since only the idealized infinite ensemble of even/odd textures has the statistical properties described above (such as identical spatial frequency spectra), it is possible that the deviation of any particular example of this ensemble from the ideal results in the asymmetric response.

Comparison of shift-register and nonshift-register stimuli

One way of testing this hypothesis is to compare responses to several examples of the ensemble. Each example must be presented several times, so that run-to-run variability in the response to a particular pattern can be compared with stimulus-dependent variations in the response. Figure 4 shows the response to four presentations of each of the three possible stimuli that can be constructed from pairs of appropriately-sized shift registers (see Appendix B and Table 1). The standard conditions of an 8.25 min check size (64 × 64 array of cells), 4.19 Hz modulation frequency, and 0.3 contrast were used. Amplitude and phase of Fourier components of the response are plotted on the complex plane, so that differences in responses correspond to distances in the plane. The fundamental components are all of approximately the same amplitude and phase. The systematic variation from stimulus (scatter on the complex plane) is not much larger than the run-to-run variability. The second-harmonic data are similar.

The motivation for basing the stimuli on shift

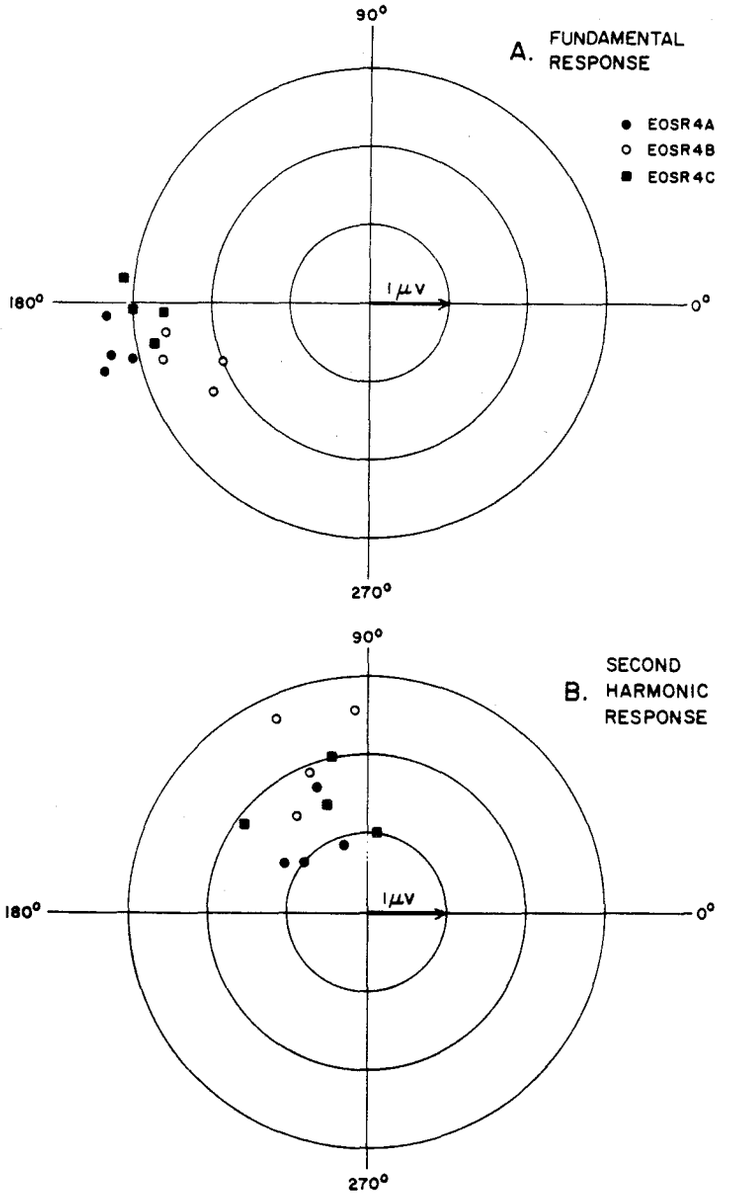

Fig. 4. Fundamental responses (A) and second harmonic responses (B) of the VEP elicited by three examples of even/odd stimuli derived from shift registers. Responses are plotted as the amplitude and phase of the Fourier components, with phase increasing in the counterclockwise direction. Stimuli are detailed in Table 1. There is a small dependence of the fundamental response on the example of the stimulus used. Subject: Y.H.

register sequences is that such stimuli would typify the ensemble (Appendix B). One might expect that responses to stimuli constructed without the use of shift registers might show a greater systematic variability. This was tested by the experiment illustrated in Fig. 5. The three even/odd textures used in this experiment were derived from a standard (PDP-11 FORTRAN) random number generator, rather than from short-cycle shift register sequences (Table 2). Although most of the responses are of similar amplitude and phase, there are clearly systematic variations of the fundamental response which exceed the run-to-run variability of the response to the individual stimuli. However, the population of fundamental responses to the random stimuli clusters about the same position in the plane as do the fundamental responses to the shift-register stimuli. The second-harmonic responses scatter independently of the choice of stimulus.

A key quantity of interest is the ratio of variance within stimulus type to total variance. If the response were independent of the example of the stimulus used, this quantity would approach unity. If the variability in the response were entirely accounted for by the choice of stimulus, this quantity would be zero. To assess whether there is any detectable dependence

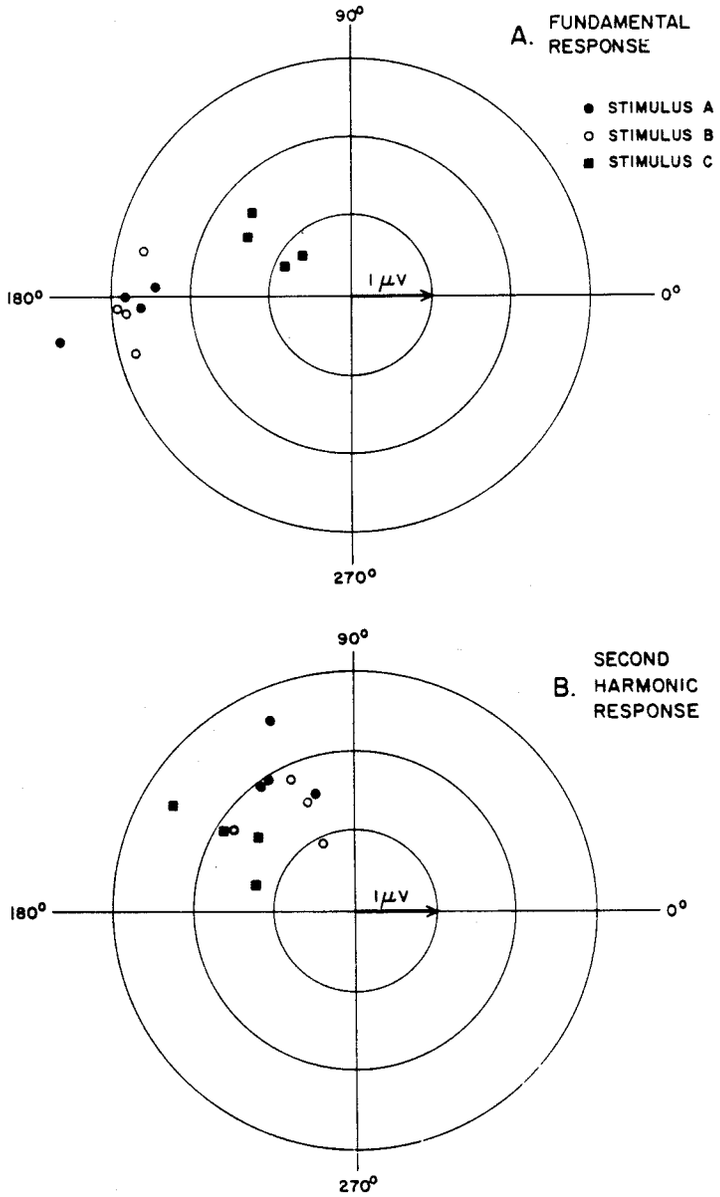

Fig. 5. Fundamental responses (A) and second harmonic responses (B) of the VEP elicited by four examples of even/odd stimuli chosen at random. Stimuli are detailed in Table 2. There is a large dependence of the fundamental response, and a small dependence of the second harmonic response, on the example of the stimulus used. Subject: Y.H.

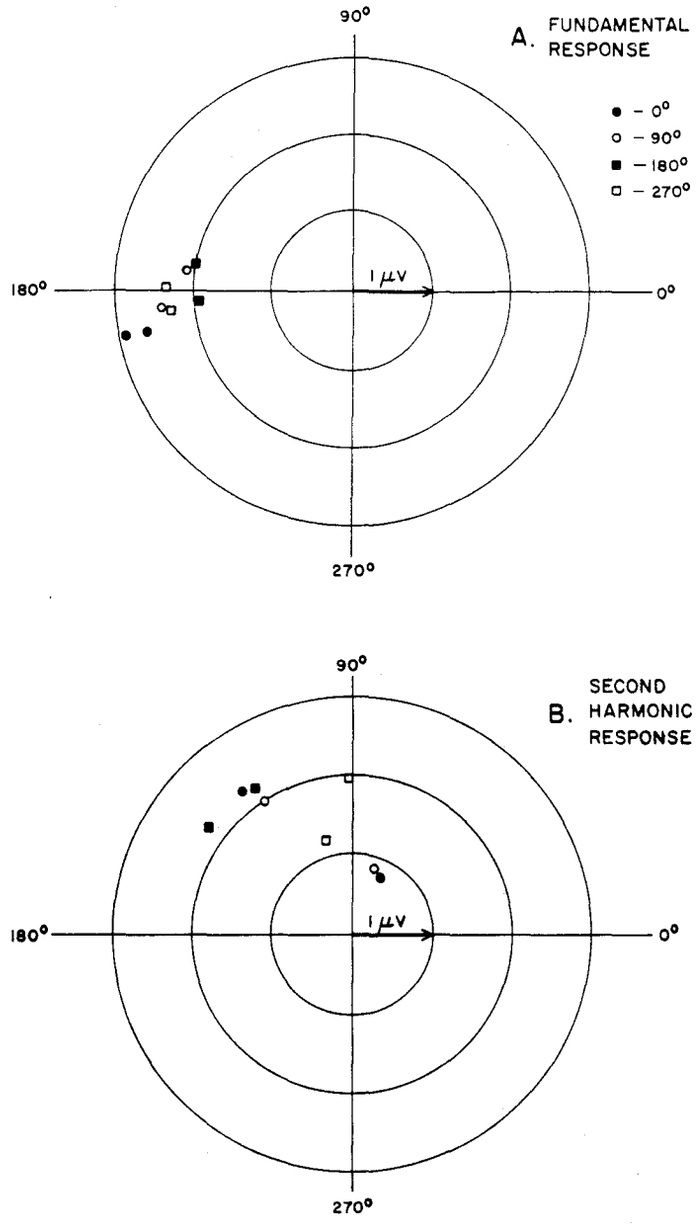

Fig. 6. Fundamental and second harmonic responses of the VEP elicited by an even/odd stimulus at four orientations. Subject: Y.H.

stimulus at four orientations 90 deg apart. Fundamental responses show a slight tendency to cluster in groups corresponding to stimulus orientation. The difference between the mean responses at two orientations is on the order of one-fifth of the size of the fundamental response, and is close to the run-to-run variability. There is no discernible dependence of second-harmonic responses on stimulus orientation.

The bootstrap variance analysis for these data is presented in Table 3. The slight dependence of the fundamental response on stimulus orientation does not reach statistical significance by this measure ($P = 0.053$). In addition, there is no significant dependence of the second harmonic response on stimulus orientation.

In another subject (M.C.), this analysis of variance suggested that a dependence of the fundamental on stimulus orientation was statistically detectable (variance ratio 0.406; $P = 0.022$). However, the difference between orientations amounted to only about one-tenth of the fundamental size, and again approached the inter-run variability.

Thus, the dependence on stimulus orientation amounts to at most a small fraction of the fundamental response. The rotated stimuli are also new examples of stimuli generated by shift-register se-

quences, and thus, the results of this experiment confirm the finding of Fig. 4 that the specific choice of stimulus plays at most a small role in determining the size of the fundamental response. Since stimulus rotation in steps of 90 deg interchanges visual information destined for right and left hemispheres, as well as superior and inferior hemifields, it is unlikely that an interaction of an asymmetry of visual processing with an asymmetry of the stimuli is primarily responsible for the observed VEP. This experiment also rules out the possibility that the anisotropy generated by the raster display plays a significant role in the VEP.

Although rotational shifts of 90 deg were expected to have no effect on the VEP and serve as a check on the methodology, rotational shifts by 45 deg might elicit different responses because of oblique effects in the visual system. Preliminary studies in three subjects failed to reveal any consistent change in the VEP related to oblique presentation, indicating that such effects are not large.

DISCUSSION

The evoked responses elicited by transition between even and odd configurations of the texture may be analyzed in terms of a symmetric component, common to both directions of transition, and an asymmetric component, which is equal and opposite at the two directions of the transition.

In terms of Fourier analysis, this decomposition amounts to assigning the fundamental and higher odd-order components to the asymmetric components and assigning the second harmonic and higher even-order harmonics to the symmetric component. In these experiments, in which local luminance is modulated sinusoidally, the only odd-order component that contained significant power was the fundamental. Therefore, the fundamental component will be equated with the asymmetric response. The symmetric component of the response usually was manifest by power in both the second and fourth-harmonic responses.

In this section, the qualitative features of mechanisms that may contribute to the asymmetric component will be discussed; analysis of the symmetric component will be pursued elsewhere in conjunction with further data on its dependence on spatial and temporal parameters of the stimulus (Victor and Zemon, 1985).

The fundamental component

The most striking aspect of the asymmetric component of the response is that it exists at all (Fig. 3). As outlined in *Stimulus description* and detailed in Appendix A, the two configurations of the stimulus are equated for luminance, local contrast (total edge length, luminance change across edges) and second- and general third-order autocorrelations. Thus, the differences in the VEP they elicit, as well as their strong perceptual differences, must rely on more complex aspects of form.

The fundamental response is not the trivial result of asymmetries

It might be argued that the statistical properties of the stimulus hold only for the infinite ensemble of textures, and therefore asymmetries in responses may reflect deviations of properties of the particular example of the stimulus from those of the ensemble. The data of Figs 4 and 5, and the analysis in Table 3, make this explanation for the bulk of the response unlikely. Fundamental responses to many different examples from the ensemble were compared; all were of a similar amplitude and phase.

There is a small tendency for VEP's elicited by different examples of the ensemble to cluster, as revealed by the fact that the within-stimulus variability was statistically less than the variation of the response between stimuli. This tendency was larger when stimuli were chosen without regard to selecting balanced sequences for the initial row and column. When shift registers are used to provide balanced sequences so that the stimuli would come close to typifying the ensemble (as described in Appendix B), averaged responses to different examples of the stimulus all have amplitudes that agree to within about 20% and phases that agree to within about 20 deg. Thus, although unavoidable aberration from statistical ideality may contribute detectably to the VEP, this does not account for the bulk of the response.

Another assumption made in the analysis is that the recording of the VEP averages local cortical activity uniformly, so that influences from different parts of the visual field contribute equally. Certainly this is not the case, as is shown by stimulation of hemifields or quadrants (Jeffreys and Axford, 1972a, b; Spekreijse *et al.*, 1973). The contribution of visual stimulation in different parts of the field must depend on the specific geometry of the appropriate cortical regions, the retinotopic map and cortical magnification factor within the regions, and the passive electrical properties of the head (Lehmann *et al.*, 1982). The data indicate that the fundamental response is unlikely to *depend* on such anisotropies or inhomogeneities of the visual system and the recording geometry. In Fig. 6, the same stimulus is used at four orientations separated by a quarter-turn. At each orientation, the amplitude and phase of the responses are substantially the same. This essentially eliminates the possibility that an interaction of anisotropies of the stimulus and anisotropies of the visual system is the source of the response. The role of translational inhomogeneities may be excluded as well. One of the properties of the textures is that translation in the plane is equivalent to choosing another texture out of the ensemble (Appendix A); above, it has been shown that the particular texture chosen is at most a weak factor in determining the VEP.

Relation to appearance/disappearance studies

There is a strong common theme between the present study and previous studies using pattern appearance and disappearance (Spekreijse *et al.*, 1973). The standard contrast-reversal checkerboard is in some sense too "symmetric" for some analytical purposes—responses that depend on local luminance, local contrast, spatial frequency, or more complex attributes of form all would lead to only even-harmonic response, and could not be qualitatively distinguished. The appearance/disappearance paradigm, in which some of the symmetry is broken, would leave unchanged luminance-dependent second harmonics, but would convert a local contrast response to the fundamental. The major fundamental response in the appearance/disappearance VEP thus provided strong evidence for a component of the VEP driven by local contrast changes.

In the present study, the symmetry of the checkerboard is broken in a different way. Is a local contrast mechanism still responsible for the fundamental component? The qualitative answer is no, but to be more quantitative, specific examples of local contrast mechanisms must be considered.

Consider first a mechanism whose receptive field is such that it is unlikely to receive input from more than two cells of the texture—for example, a small slit. In both configurations of the texture, exactly half of neighboring cell pairs are of equal luminance, and the rest all have the same luminance difference. The number of transitions between each possible kind of cell pair is independent of whether the texture is changing from even to odd or vice-versa (Victor and Zemon, 1984). Hence, no amount of temporal processing (linear or nonlinear) can extract an asymmetric component from population responses generated within the constraints of such receptive fields. A similar argument holds for receptive fields that include three cells of the texture (Appendix A, Theorem III). Thus, any mechanism which generates an asymmetric response to the even/odd stimuli must receive input from more than three cells of the texture.

Consider next mechanisms of arbitrary spatial structure, but in which nonlinearities are of at most third order. This category includes a purely multiplicative interaction between two or three linearly-summing pools. The category also includes a mechanism which consists of linear summation according to any point-weighting function, followed by a square-law device. The even and odd configurations of the stimuli have identical first-, second-, and third-order correlation statistics (Appendix A, Theorem IV). This identity implies that the mean output of any such mechanism will be the same, averaged over the ensemble of even or odd patterns.

As a simple example, consider a mechanism which sums light over a 2×2 patch of the stimulus, and then applies a power-law nonlinearity. Assume that the light intensity of the bright squares is L, and of the dark squares is $-L$. In the even texture, 1/8 of the patches have total intensity $4L$ (four light cells), 1/8 of the patches have total intensity $-4L$ (four dark cells), and 3/4 of the patches have total intensity 0 (two light cells and two dark cells). In the odd texture, 1/2 of the patches have total intensity $2L$ (three light cells and one dark cell) and 1/2 of the patches have total intensity $-2L$ (one light cell and three dark cells).

Now compare the responses of a power-law nonlinearity averaged over these two distributions of inputs. A first-power (linear) device will have an average output of 0 for both even and odd textures. A second-power (quadratic) device will have an average output of $4L^2$ for both textures. A third-power (cubic) device will have an average output of 0 for both textures. Only fourth-power and higher even-power nonlinearities of this sort would have different outputs when averaged over the two textures. This is a consequence of Theorem IV in Appendix A. More generally, any mechanism which generates an asymmetric response to the even-odd stimuli must possess nonlinearities of formal order at least four, and must receive input from at least four cells of the texture.

A simple mechanism sensitive to local contrast would consist of the square of the difference in output of two neighboring pools. This mechanism, when applied to appearance/disappearance stimuli, will produce a strong fundamental response: at pattern appearance, contribution from all edges will reinforce; at pattern disappearance, there will be no response from this mechanism. Such a mechanism, which may receive input from only two cells of the texture and is of formal order two, does not fulfill either requirement needed to explain the asymmetric response observed here. This fundamental component requires a mechanism with greater spatial and dynamical complexity.

Rectifying subunits are not robust generators of the fundamental response

The preceding analysis may be summarized: a mechanism which generates the fundamental component in response to even-odd stimuli requires input from at least four cells of the texture and a nonlinearity of formal order at least four. One possibility for such a mechanism is multiplication of light input from four cells in a two-by-two patch. This hypothesis is unattractive because this quadruple-product interaction seems rather unphysiologic, and because it predicts that the strength of the fundamental response would grow as the fourth power of the overall stimulus contrast, while a much more gentle dependence is observed (Victor and Zemon, unpublished data).

One highly nonlinear element, sharp rectification, is well-documented in the mammalian visual system (Spekreijse *et al.*, 1973; Victor and Shapley, 1979). A rectifier (full-wave or half-wave) certainly will generate nonlinear components of all even orders, at least formally. If rectification is the only nonlinearity in an

otherwise linear system, then the response size will be proportional to stimulus contrast (although the other criterion of linearity, superposition, will be violated).

Thus, one specific model which might generate a fundamental response which grows approximately proportionally with contrast is a neural mechanism which sums light intensity over a 2×2 region of the texture, and rectifies the result. More generally, any model mechanism which includes a rectified signal from linear pooling of at least four cells of the texture will be a candidate for a generator of the fundamental component. For example, the Y cell receptive field is well-modelled by a superposition of many rectifying subunits on a traditional center/surround (Hochstein and Shapley, 1976; Victor and Shapley, 1979). It has recently been shown that the receptive-field properties of many primary visual cortex cells are concisely explained by linear combination of the outputs of a small number of rectifying subunits (Spitzer and Hochstein, 1984a, b).

Will the fundamental component generated by such models in response to these isodipole stimuli be robust? If there are no additional nonlinear spatial interactions, the fundamental component generated by such neurons must rely on differences in the distributions of output of the rectifying subunits. This difference was determined empirically by a Monte Carlo simulation (Fig. 7). The average output of a subunit that sums light linearly over a circular region and rectifies the result is plotted as a function of subunit size. For most subunit sizes, a conservative estimate of the difference of the average response to the even and odd configurations is about 15% of the total response. For a narrow range of subunit sizes, in which the subunit radius is matched to the size of the texture cell, this disparity reaches 30%. The disparity is not substantially changed when the rectifier is followed by a fractional-power device of power 0.5 or 1.5. Additional calculations showed that similar results hold for square and rectangular subunit shapes.

In the data shown here (Fig. 3), the fundamental component is at least as large as the second-harmonic component. In addition, the fundamental and second-harmonic components have distinct spatio-temporal dependences (Victor and Zemon, 1984, 1985). Thus, it is unlikely that the fundamental response is generated solely by a mechanism to which even and odd configurations appear the same to within 15% at most spatial scales. The implication of

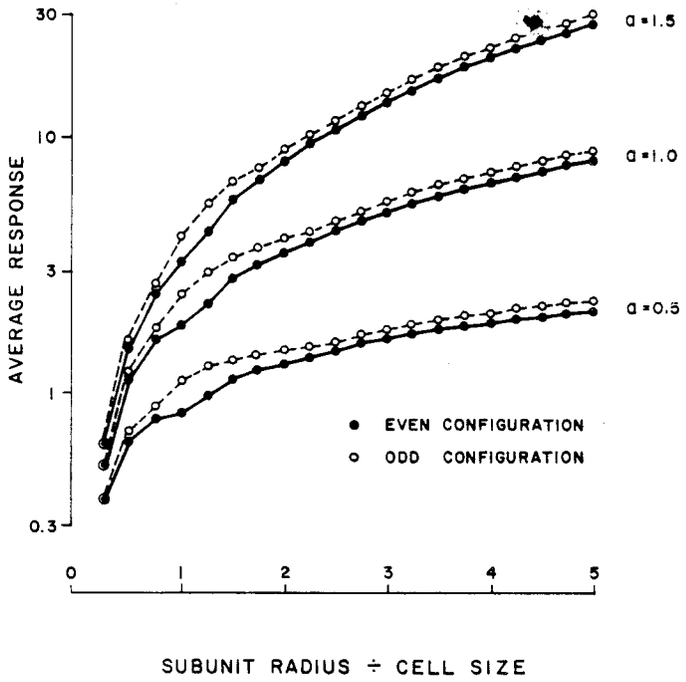

Fig. 7. Comparison of calculated population responses of circular rectifying subunits to even and odd configurations. For each data point, the mean output of 10,000 such subunits placed at random on an infinite sample of the texture is calculated. The output of a single subunit is generated by convolving the subunit profile with a function representing the deviation of the luminance of the stimulus from the mean. Points of the stimulus with luminances above the mean are assigned a value of $+1$; luminances below the mean correspond to -1. (The inclusion of a constant offset would only reduce the effect of the nonlinearity and decrease the disparity between even and odd textures.) This pooled signal is then transformed by a power-law rectifier $y = x^a$. Full-wave rectification is used, because half-wave rectification would merely halve the response to both even and odd textures, since the pooled signals are always symmetrically distributed about zero. For subunits whose diameter is approximately that of the texture cell, mean responses to even and odd textures differ by about 30%. For other subunit sizes, the difference is much smaller. This disparity does not depend on the choice of the exponent a.

this analysis for modelling generators of the asymmetric component of the response is: a linear superposition of rectifying subunits (such as the receptive-field model of Spitzer and Hochstein) without additional nonlinear spatial interactions is not likely to produce the responses observed. The rectifying subunit, either retinal or cortical, may play a role in the generation of this response, but additional nonlinear interactions are required.

It must be stressed that although this analysis indicates that the rectifying subunit is probably not the generator of this fundamental response, one cannot conclude that the fundamental responses elicited by the appearance/disappearance stimulus and the even/odd stimulus are entirely distinct. Rather, any mechanism which contributes to the fundamental response to the present stimulus will in general also generate a fundamental response to appearance/disappearance. This analysis does indicate that the VEP contains components reflecting complex visual processing. These components, which are likely present in the response to more standard stimuli as well, may be isolated by manipulation of the spatial properties of the stimulus.

Acknowledgements—I thank Mary Conte, Dr Jim Gordon, Yvonne Holland, Norman Milkman, Michelangelo Rossetto, and Gary Schick for their excellent technical assistance. I thank Drs Bruce Knight, Floyd Ratliff, Robert Shapley, and Vance Zemon for their many helpful suggestions. The time willingly spent by these members of the Biophysics Laboratory as subjects is gratefully appreciated. This work was supported in part by grants EY188, EY2439, EY5466, and NS877 from the National Institutes of Health, The Harry Frank Guggenheim Foundation, and The Klingenstein Fund. J.V. is a Hartford Fellow and received additional support from the The McKnight Foundation.

REFERENCES

Celesia G. G. (1982) Clinical applications of evoked potentials. In *Electroencephalography* (Edited by Niedermeyer E. and Lopes da Silva F. M.), pp. 665–684. Urban & Schwartzenberg, Baltimore, Md.

Chiappa K. H. and Ropper A. H. (1982) Evoked potentials in clinical medicine. Part I. *New Engl. J. Med.* **306,** 1140–1150.

Creutzfeldt O. D. and Kuhnt U. (1973) *Handbook of Sensory Physiology* (Edited by Jung R.), Vol. 7, Part 3, pp. 595–646. Springer, Berlin.

Creutzfeldt O. D., Rosina A., Ito M. and Probst W. (1969) Visual evoked responses of single cells and of the EEG in primary visual areas of the cat. *J. Neurophysiol.* **32,** 127–139.

Efron B. (1980) The jacknife, the bootstrap, and other resampling plans. Technical report no. 63, Division of Biostatistics, Stanford University, Stanford, Calif. ii + 135 PP.

Golomb S. W. (1968) *Shift Register Sequences*. Holden-Day, San Francisco, Calif.

Hochsten S. and Shapley R. (1976) Linear and nonlinear spatial subunits in Y cat retinal ganglion cells. *J. Physiol.* **262,** 265–284.

Jeffreys D. A. and Axford J. G. (1972a) Source locations of pattern-specific components of human visual evoked potentials. I. Component of striate cortical origin. *Expl Brain Res.* **16,** 1–21.

Jeffreys D. A. and Axford J. G. (1972b) Source locations of pattern-specific components of human visual evoked potentials. II. Component of extrastriate cortical origin. *Expl Brain Res.* **16,** 22–40.

Julesz B., Gilbert E. N. and Victor J. D. (1978) Visual discrimination of textures with identical third-order statistics. *Biol. Cybernet.* **31,** 137–140.

Lehmann D., Darcey T. M. and Skrandies W. (1982) Intracerebral and scalp fields evoked by hemiretinal checkerboard reversal, and modeling of their dipole generators. *Adv. Neurol.* **32,** 41–48.

Milkman N., Schick G., Rossetto M., Ratliff F., Shapley R. and Victor J. (1980) A two-dimensional computer-controlled visual stimulator. *Behav. Res. Meth. Instrum.* **12,** 283–292.

Nakayama K. (1982) The relationship of visual evoked potentials to cortical physiology. *Ann. N.Y. Acad. Sci.* **388,** 21–36.

Nunez P. L. (1981) *Electric fields of the Brain*, 484 pp. Oxford Univ. Press.

Regan D. (1972) *Evoked Potentials in Psychology, Sensory Physiology, and Clinical Medicine*. Wiley, New York.

Spekreijse H., Estevez O. and Reits D. (1977) Visual evoked potentials and the physiological analysis of visual processes in man. In *Visual Evoked Potentials in Man* (Edited by Desmedt J. E.), pp. 16–89. Clarendon Press, Oxford.

Spekreijse H., Van der Tweel L. H. and Zuidema T. (1973) Contrast evoked responses in man. *Vision Res.* **13,** 1577–1601.

Spitzer H. and Hochstein S. (1984a) Simple and complex cell response dependences on stimulus parameters. *J. Neurophysiol.*

Spitzer H. and Hochstein S. (1984b) A complex cell receptive field model. *J. Neurophysiol.*

Tyler C. W. and Apkarian P. A. (1982) Properties of localized pattern evoked potentials. *Ann. N.Y. Acad. Sci.* **388,** 662–670.

Tyler C. W., Apkarian P. A. and Nakayama K. (1978) Multiple spatial frequency tuning of electrical responses from the human visual cortex. *Expl Brain Res.* **33,** 535–550.

Vaughan H. G. Jr (1982) The neural origins of human event-related potentials. *Ann. N.Y. Acad. Sci.* **388,** 125–138.

Victor J. D. and Shapley R. (1979) The nonlinear pathway of Y ganglion cells in the cat retina. *J. gen. Physiol.* **74,** 671–689.

Victor J. D. and Zemon V. (1984) Separation of components of the pattern VER using complex visual textures. *Proc. 6th Ann. Conf. I.E.E.E. Engineering in Medicine and Biology Society*, pp. 420–425.

Victor J. and Zemon V. (1985) The human visual evoked potential: analysis of components due to elementary and complex aspects of form. *Vision Res.* **25,** 1829–1842.

Zemon V., Kaplan E. and Ratliff F. (1980) Bicuculline enhances a negative component and diminishes a positive component of the visual evoked cortical potential in the cat. *Proc. natn. Acad. Sci. U.S.A.* **77,** 7476–7478.

Zemon V. and Ratliff F. (1982) Visual evoked potentials: evidence for lateral interactions. *Proc. natn. Acad. Sci. U.S.A.* **79,** 5723–5726.

Zemon V. and Ratliff F. (1984) Intermodulation components of the visual evoked potential: responses to lateral and superimposed stimuli. *Biol. Cybernet.* **50,** 401–408.

APPENDIX A: PLANE MARKOV PROCESS TEXTURES

This appendix contains a brief but rigorous discussion of the statistical properties of the textures that form the basis of the present class of visual stimuli. These "even" and "odd" textures, introduced by Julesz and coworkers (1978), are best considered as part of a larger class of isodipole textures, to be called plane Markov process (PMP) textures. This

added generality provides more insight into the underlying properties of the textures, suggests possibilities for further experiments, and carries little additional complexity.

Definition of the PMP textures

Each texture consists of a tessellation of the plane into square cells, and a stochastic rule for assigning one of two texture elements to each cell. Call the cell in the ith row and jth column $A_{i,j}$. The texture element assigned to the cell $A_{i,j}$ will be denoted by $a_{i,j}$. In the textures of Fig. 1, $a_{i,j} = +1$ signifies an unfilled cell, and $a_{i,j} = -1$ signifies a stippled cell.

The textures of Fig. 1 are the extreme elements of a continuous family of textures, characterized by a parameter c. This parameter can have any value from -1 to 1: when $c = +1$, the even texture of Fig. 1 is generated; when $c = -1$, the odd texture of Fig. 1 is generated; when $c = 0$, the texture consists of random assignments of the squares to intensities ± 1. For an arbitrary value of c, the textures are generated as follows: first, assign texture elements to each of the squares $A_{0,j}$ and $A_{i,0}$ randomly and independently, so that each square has a probability of 1/2 of containing either texture element. Next, texture elements are assigned to squares not in the initial row or column according to the following recursive rule

$$\text{prob}(a_{i,j} \cdot a_{i-1,j} \cdot a_{i,j-1} \cdot a_{i-1,j-1} = 1) = (c+1)/2. \quad \text{(A1)}$$

That is, the probability that the number of cells with either texture element in every 2×2 block of adjacent cells is *even* is given by $(c+1)/2$. In the case $c = +1$, the number of such cells *must* be even. In the case $c = -1$, the number of such cells *must* be odd. In these two deterministic cases, the probabilistic rule (A1) reduces to equation (1) of the text.

A non-recursive rule for the deterministic textures

For the deterministic textures, the recursion rule can be iterated to generate an explicit formula for the general $a_{i,j}$ in terms of the states of the squares in the initial row and column. More generally

Theorem I: For textures with $c = \pm 1$

$$a_{i,j} = a_{i-I,j} \cdot a_{i,j-J} \cdot a_{i-I,j-J} \cdot c^{IJ}. \quad \text{(A2)}$$

The proof is by double induction on I and J. The definition (A1) proves (A2) for $I = 1$ and $J = 1$. Assume now that (A2) holds for $1 \le I \le I_0 - 1$ and $1 \le J \le J_0$; we will demonstrate (A2) for $I = I_0$. By hypothesis

$$a_{i,j} = a_{i-I_0+1,j} \cdot a_{i,j-J_0} \cdot a_{i-I_0+1,j-J_0} \cdot c^{(I_0-1)J_0}. \quad \text{(A3)}$$

Now, apply (A2) to the first term of the product of (A3) with $I = 1$ and $J = J_0$

$$a_{i-I_0+1,j} = a_{i-I_0,j} \cdot a_{i-I_0+1,j-J_0} \cdot a_{i-I_0,j-J_0} \cdot c^{J_0}.$$

Substitution of this for the first term in (A3) leads to

$$a_{i,j} = a_{i-I_0,j} \cdot a_{i,j-J_0} \cdot a_{i-I_0,j-J_0} \cdot c^{I_0 J_0}$$

which extends the induction in the I-direction. A similar argument extends the induction in the J-direction, which establishes (A2).

Text equation (2) follows by taking $i = I$, $j = J$ in Theorem I:

$$a_{i,j} = a_{0,j} \cdot a_{i,0} \cdot a_{0,0} \cdot c^{ij}. \quad \text{(A4)}$$

An important consequence is

Theorem II: an even texture ($c = +1$) can be converted to an odd texture ($c = -1$) by reversing the states of all cells whose row number and column number are both odd.

Correlation properties of the deterministic textures

The relation (A4) suffices to determine the Nth-order correlations among cells of the deterministic ($c = \pm 1$) textures. Consider N arbitrary distinct cells $A_{i_1,j_1}, \ldots, A_{i_N,j_N}$. When is the total number of such cells which contain one kind of texture element restricted? Because of the rule for texture generation, any restriction must refer only to whether this total can be even or odd. Thus, it suffices to determine whether the value of the product

$$P = a_{i_1,j_1} \cdot \ldots \cdot a_{i_N,j_N}$$

is restricted.

Using (A4), this product expands to

$$P = (a_{i_1,0} \cdot \ldots \cdot a_{i_N,0}) \cdot (a_{0,j_1} \cdot \ldots \cdot a_{0,j_N}) \cdot a_{0,0}^{N} \cdot c^{i_1 j_1 + \ldots + i_N j_N}$$

Since the elements $a_{i,0}$ and $a_{0,j}$ are uncorrelated, the above product may be free to have either value ± 1 unless it vanishes identically. This requires that the $a_{i,0}$'s and the $a_{0,j}$'s cancel each other in pairs.

Therefore,

Theorem III: the cells $S = \{A_{i_1,j_1}, \ldots, A_{i_N,j_N}\}$ are uncorrelated unless every row and column of the texture contains an even number (or possibly zero) of these cells. In this case, for the $(c = +1)$ – texture, the number of such cells in both states must be even; for the $(c = -1)$ – texture, the parity of the number of cells in either state must be equal to the parity of $i_1 j_1 + \ldots + i_N j_N$.

Correlation properties of the nondeterministic textures ($-1 < c < 1$) are only slightly more complex. The same rule, Theorem III, serves to define the situations in which states of cells are uncorrelated. However, when correlations occur, the strength of the correlation depends on the distances between the cells and on c.

Certain crucial results now follow readily. Because Theorem III requires at least four cells to obtain nonzero correlations, we recover the result of Julesz *et al.* (1978):

Theorem IV: the second- and third-order correlation functions of the deterministic textures generated by equation (A1) are zero.

Theorem III guarantees that there are no correlations among any of the cells of any single row and column pair. This means that any row/column pair could have been used equally well in place of the row and column initially used in the definition of the textures. Thus, the PMP textures are homogeneous in a statistical sense: translation of the origin of a PMP texture is equivalent to choosing a new set of values for the index rows and index columns.

Generalizations of the PMP textures

There are a number of simple generalizations of these textures which preserve the critical feature of equal second-order statistics, and consequently indentical spatial power spectra. These generalizations may prove useful in further studies of the properties of mechanisms that contribute to the VEPs studied above.

The cells $A_{i,j}$ may be filled with any pair of texture elements (not just homogeneous bright and homogeneous dark) depending on the values of the $a_{i,j}$. Thus, $a_{i,j} = 1$ could indicate a diagonal line drawn from upper left to lower right within a cell, and $a_{i,j} = -1$ could indicate a diagonal line drawn from lower left to upper right. Alternatively, the texture elements that fill $A_{i,j}$ may be derived stochastically from the states $a_{i,j}$. For example, $a_{i,j} = 1$ could indicate that $A_{i,j}$ is bright with probability $1 - e$ and dark with probability e, and $a_{i,j} = -1$ could indicate that $A_{i,j}$ is bright with probability e and dark with probability $1 - e$. Second- and third-order correlations are absent, and fourth-order correlations depend both on c and e.

The PMP textures can also be generalized by allowing them to be transformed by a linear spatial filter. This operation preserves the equality of second- and third-order correlation functions. The importance of this observation is that blur due to imperfect optics does not destroy the identity of second- and third-order correlation functions of texture pairs generated by these methods.

APPENDIX B: CHOICE OF INITIAL ROW AND COLUMN

Formally, the procedures for texture generation we have described create an ensemble of textures. A choice of a particular initial row and column will select an example from the ensemble. The statistical properties of the ensemble discussed in Appendix A will only be approximated by the statistics of any particular example. Thus, it is desirable to choose examples from the ensemble which in some sense typify the ensemble's properties.

For this reason, most of the experiments reported here have used linear binary shift register sequences (LBSRS's) to generate the initial rows and columns. An LBSRS of order k is a cycle of $N_k = 2^k - 1$ binary digits with several remarkable properties (Golomb, 1968). Within this cycle, every possible k-tuple of 0's and 1's occurs exactly once, except for the sequence of k 0's, which does not occur at all. Thus, over a spatial scale of k, this sequence essentially matches the ensemble ideal of uniform sampling of all sequences of 0's and 1's. Furthermore, over all distances (except the cycle length itself), the pairwise correlation is $\pm 1/N_k$. Thus, the autocorrelation function is essentially zero except at distances equal to repeats of the cycle.

For each $k \geq 5$, several LBSRS's exist. Each LBSRS is described by an irreducible polynomial in x of degree $k + 1$ over Z_2, which defines a Galois field of size 2^k. The jth element of the LBSRS is the constant coefficient of x^j in this Galois field. The defining polynomials used and the LBSRS's they generate are shown in Table 1.

A pair of such LBSRS's were used to construct each example of the even texture. (If necessary, 0's for 1's were interchanged in one of the LBSRS's so that the sequences concur at $a_{0,0}$). The resulting texture has a repeating unit of size $N_k \times N_k$. Every possible $k \times k$ patch of the even texture will occur exactly twice in this repeating unit, with the exception of blocks which are uniform along one or both dimensions. Blocks uniform along one dimension will all occur exactly once per repeat, and only one uniform $k \times k$ block (black or white but not both) will occur in each repeat. This follows from the nonrecursive definition of the textures [text equation (2)]. Thus, over small spatial distances, this even texture approximates the properties of the ensemble of even textures at all orders.

Furthermore, the (second-order) autocorrelation of this texture at large distances is well-behaved and small. For displacements parallel to an axis, the autocorrelation is given by that of the underlying LBSRS. For displacements parallel to neither axis, the autocorrelation is the product of the autocorrelations at displacements equal to the projection of the original displacement on the two axes. Thus, for typical displacements not equal to a repeat length, the autocorrelation is $\pm 1/(N_k)^2$. For displacements along one axis (but not a repeat length), the autocorrelation is $\pm 1/N_k$, and for displacements equal to a repeat period, the autocorrelation is 1. This is quite close to ideal behavior.

A finite sample of this texture containing approximately two repeat periods along each axis will have these properties in an approximate sense and will not appear periodic to casual inspection (Fig. 2). The LBSRS, which is intrinsically cyclic, is broken with a phase so that no large uniform block is near the fixation point.

The benefit of retaining two repeats of the LBSRS along each axis becomes apparent when the transition to the odd texture is made. Because of the *odd* length of the LBSRS, alternate repeats of each LBSRS are treated differently [text equation (2)]. Thus, each of the four possible ways that a $k \times k$ block of an even texture can be converted to a block of an odd texture (depending on the parity of the coordinates of its position along the two axes) occurs the same number of times.